

Electronic Supplementary Information (ESI) for

Growth of Close-Packed Crystalline Polypyrrole on Graphene Oxide via *in situ* Polymerization of Two-Monomer-Connected Precursor

Wonbin Kim^{1,†}, Hong-Joon Lee^{1,†}, Zubair Ahmad¹, Seung Jo Yoo^{2,3}, Youn-Joong Kim², Santosh Kumar¹, Mohammad Changez^{1,4}, Jung-Soo Lee⁵ and Jae-Suk Lee^{1*}

¹School of Materials Science and Engineering, Gwangju Institute of Science and Technology (GIST), 123 Cheomdangwagi-ro, Buk-gu, Gwangju 61005, Korea

²Electron Microscopy Research Center, Korea Basic Science Institute (KBSI), 169-148 Gwahak-ro, Yuseong-gu, Daejeon 34133, Korea.

³Department of Materials Science and Engineering, Korea Advanced Institute of Science and Technology (KAIST), 291 Daehak-ro, Yuseong-gu, Daejeon 34141, Korea.

⁴Department of Basic Sciences, College of Applied Sciences, A'Sharqiyah University, Ibra 400, Oman

⁵Department of Bio-chemical and Polymer engineering, Chosun University, 309 Pilmun-daero, Dong-gu, Gwangju 501-759, Korea.

[†]These authors contributed equally to this work

*Corresponding Author. E-mail: jslee@gist.ac.kr

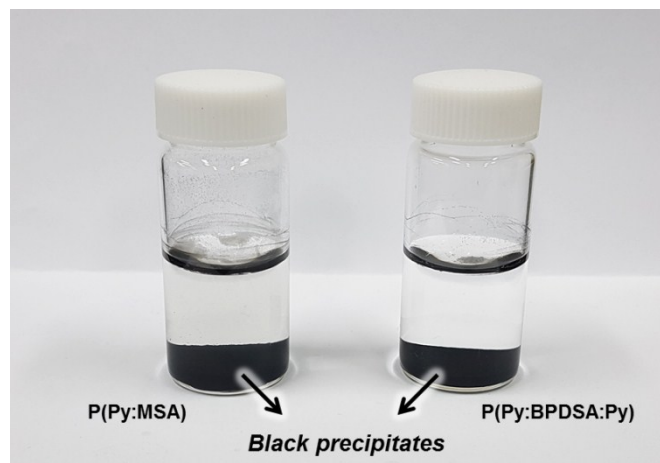


Fig. S1 Photographs of precipitated P(Py:MSA) and P(Py:BPDSA:Py). Black precipitates were obtained on the bottom of reactors.

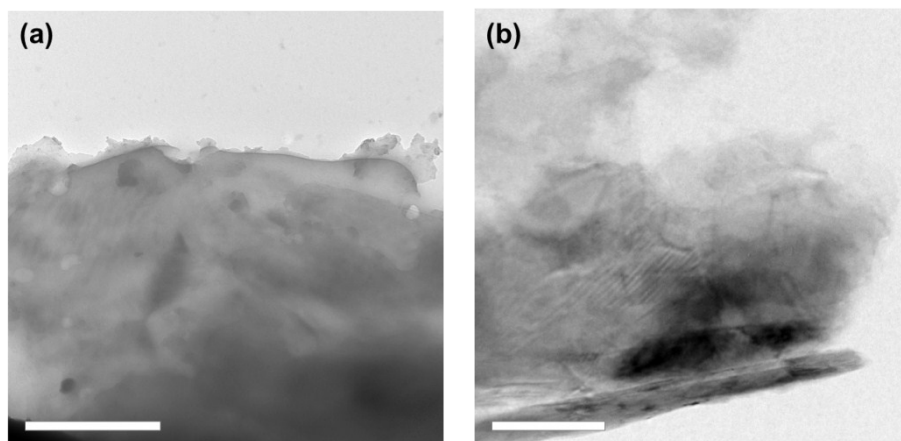


Fig. S2 (a) TEM micrographs at a low magnification of P(Py:MSA) and (b) P(Py:BPDSA:Py). Scale bar, 1 μm . Bulk aggregations were observed without 2D graphene oxide templates.

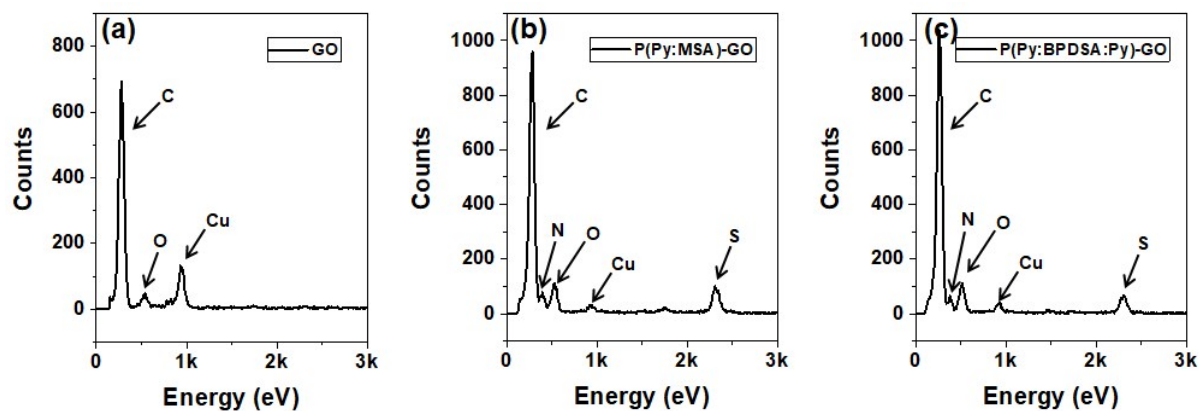


Fig. S3 EDS graphs of GO and composites. (a) GO, (b) P(Py:MSA)-GO. (c) P(Py:BPDSA:Py)-GO. The EDS was measured at the same region with each TEM image in Figure 2a-c. N and S elements detected in the composites were only from Py units and sulfonic acids of the *in situ* synthesized polymers on GO. Cu peaks were detected from copper TEM grids.

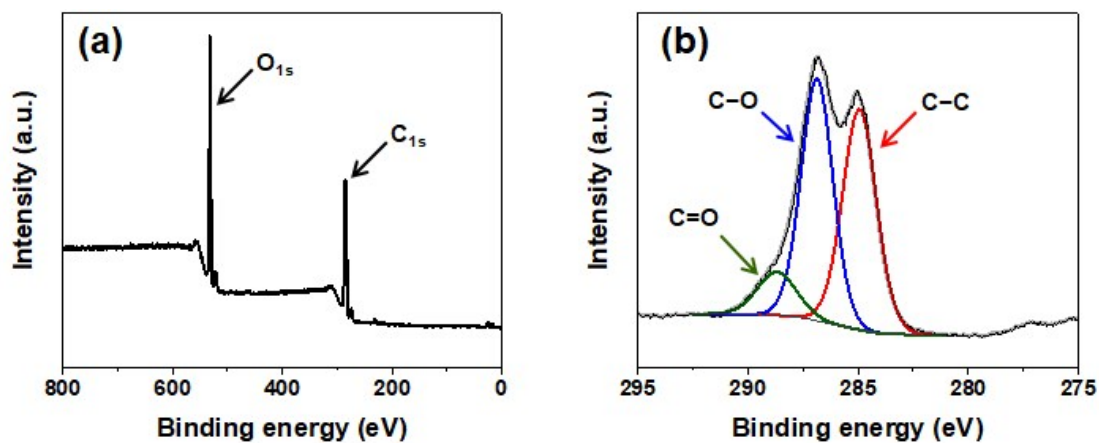


Fig. S4 XPS spectra of GO. (a) Full spectrum. (b) C_{1s} signals. GO composed of only C and O (atomic percent, 68.15 and 31.85 %, respectively). In C_{1s} signals, three components were observed for C-C (284.9 eV), C-O (286.8 eV) and C=O (288.6 eV).¹

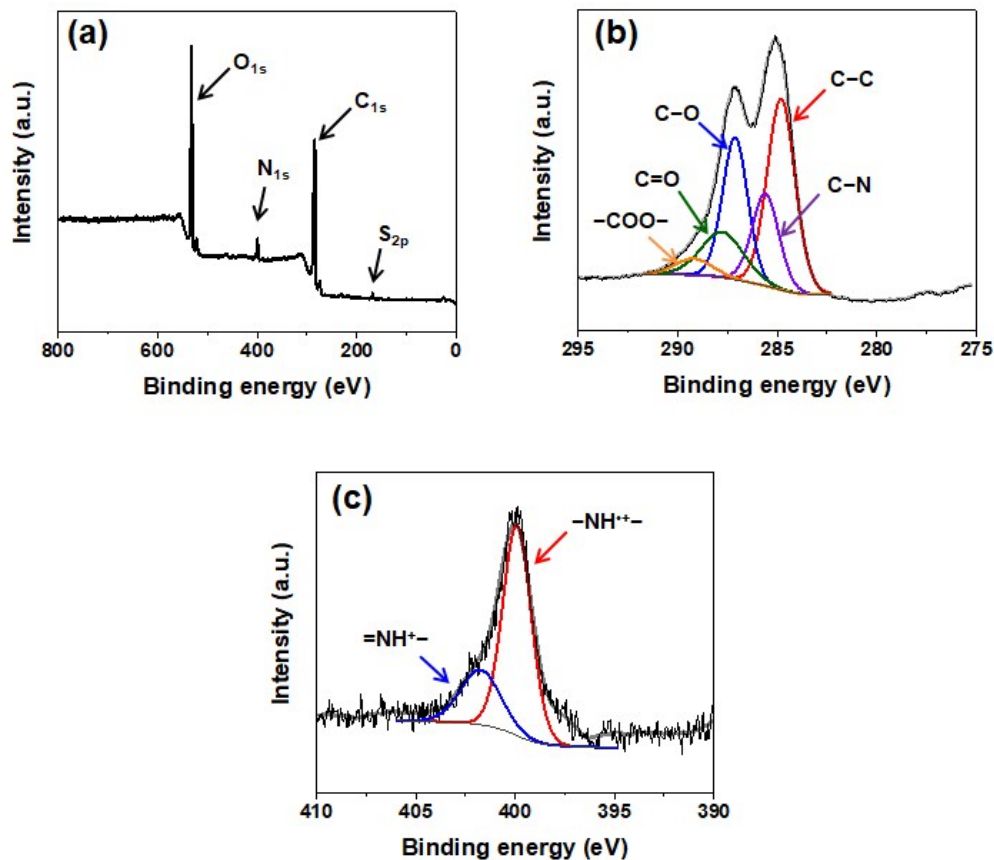


Fig. S5 XPS spectra of P(Py:MSA)-GO. (a) Full spectra. (b) C_{1s} signals. (c) N_{1s} signals. P(Py:MSA)-GO composed of C, O, N and S elements (Atomic percent, 69.5, 25.0, 4.3 and 1.2 %, respectively). In C_{1s} signals, five components were observed for C-C (284.8 eV), C-N (285.6 eV), C-O (287.1 eV), C=O (287.8 eV) and -COO- (289.2 eV).¹ The N_{1s} signals show mostly the charged nitrogen components at 400.0 and 401.7 eV, which correspond to -NH⁺⁻ and =NH⁺⁻, respectively.^{1, 2} The positively charged nitrogen was formed by ionic interaction with sulfonic acid groups of MSA.

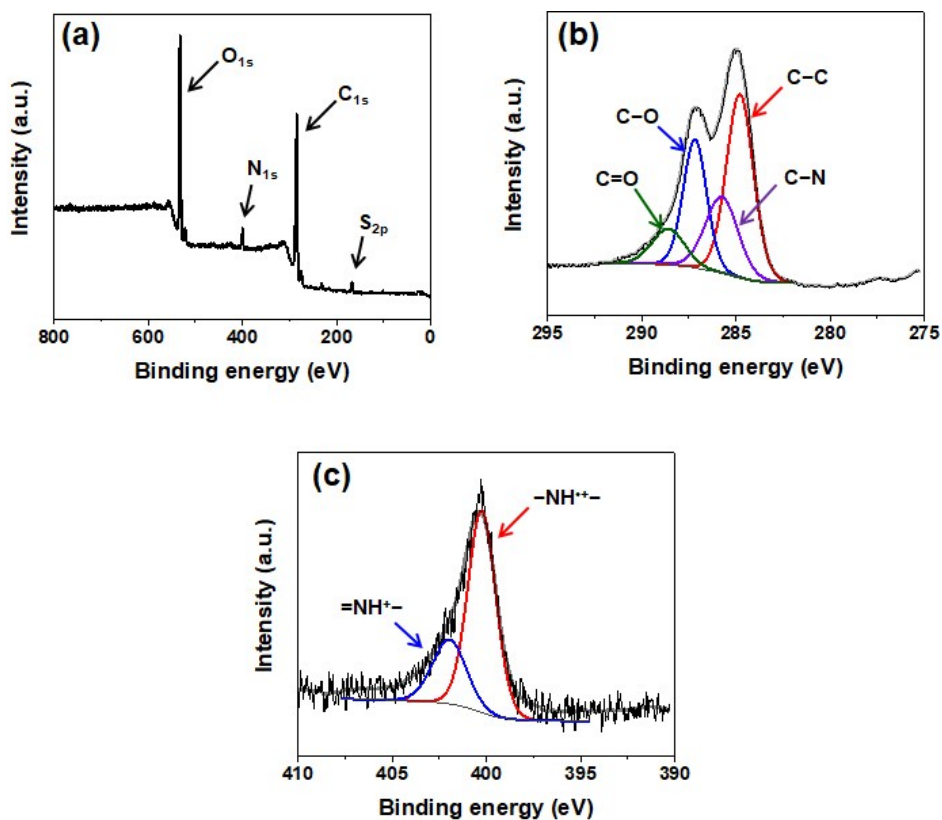


Fig. S6 XPS spectra of P(Py:BPDSA:Py)-GO. (a) Full spectrum (b) C_{1s} signals. (c) N_{1s} signals. Similar to the composites of P(Py:MSA)-GO, P(Py:BPDSA:Py)-GO composed of C, O, N and S elements (Atomic percent, 69.8, 24.1, 4.0 and 2.1 %, respectively). In C_{1s} signals, four components also were observed for C-C (284.8 eV), C-N (285.8 eV), C-O (287.1 eV) and C=O (288.6 eV).¹ The N_{1s} signals show the charged nitrogen components at 400.2 and 401.9 eV, corresponding to -NH⁺⁻ and =NH⁺⁻, respectively.^{1, 2} The positively charged nitrogen was made by ionic interaction with sulfonic acid groups of BPDSA connectors.

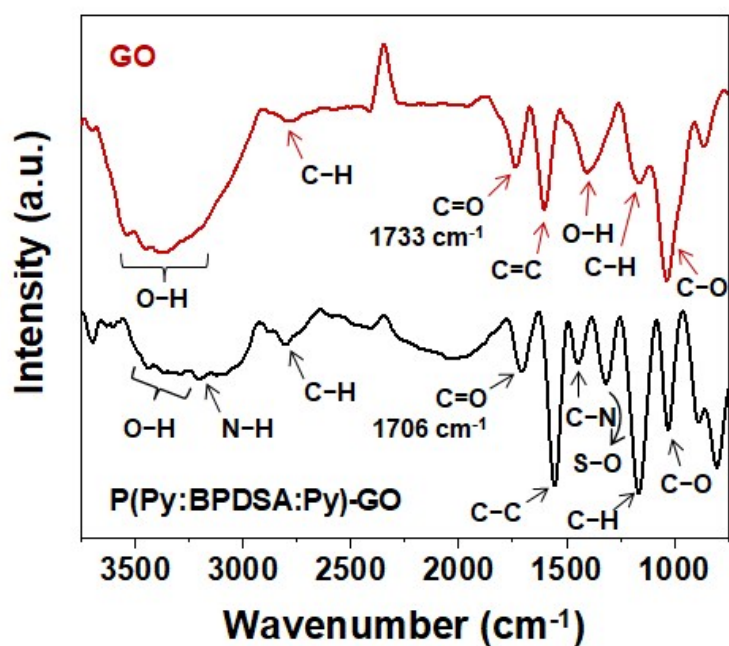


Fig. S7 FT-IR spectra of GO and P(Py:BPDSA:Py)-GO. In the spectrum of GO, a strong and broad absorption is observed at near 3300 cm^{-1} , which is attributed to the vibration of O-H.³ Also, the spectrum shows the stretching and bending of C-H (2805 and 1162 cm^{-1}) and a graphitic C=C (1602 cm^{-1}).³ In the spectrum of P(Py:BPDSA:Py)-GO composite, the characteristic peaks of PPy with sulfonate groups were observed such as the stretching vibration of N-H (3208 cm^{-1}), C-N (1440 cm^{-1}), and S-O (1317 cm^{-1}).^{3, 4} The most important phenomena in these two spectra are that the stretching vibration of C=O is shifted from 1733 (GO) to 1706 cm^{-1} (composite), demonstrating the existence of strong hydrogen bonding between polymer and GO.¹

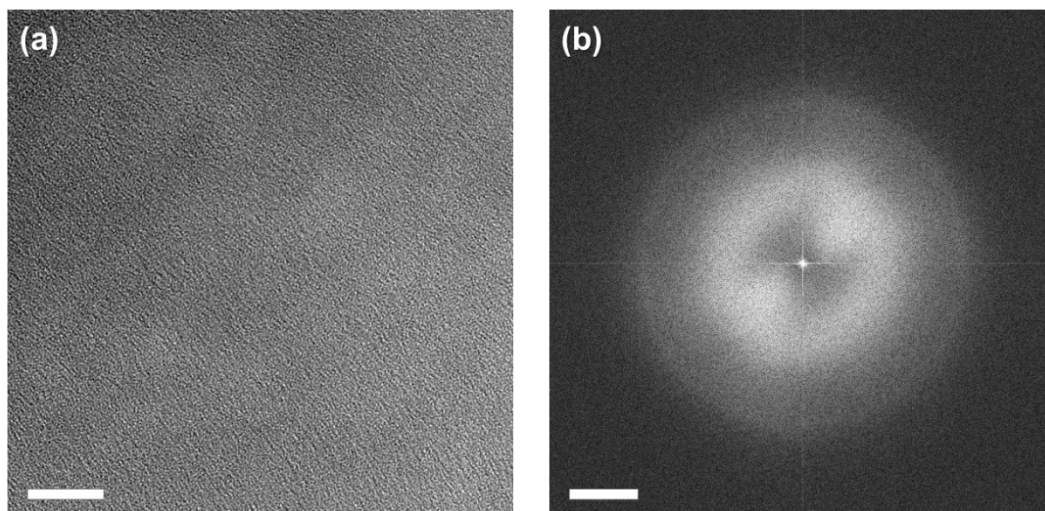


Fig. S8 (a) HRTEM image of P(Py:MSA)-GO. (b) The corresponding FFT pattern image of (a).

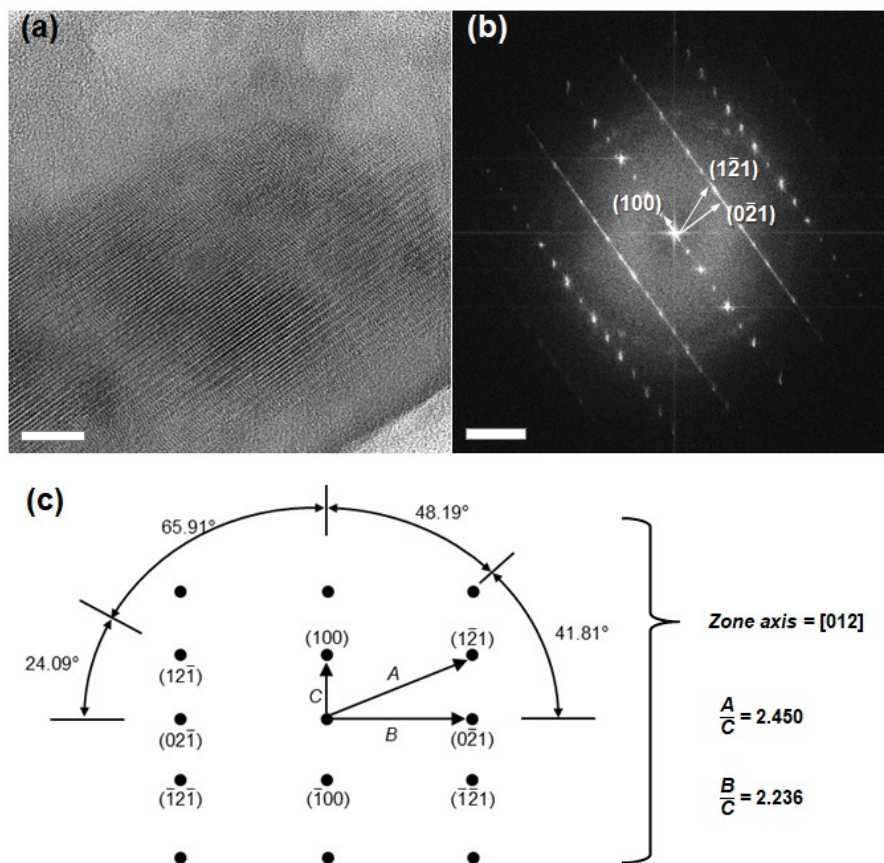


Fig. S9 Crystal structure analysis. (a) HRTEM and (b) FFT pattern image of P(Py:BPDSA:Py)-GO. Scale bars, 10 nm, and 2 nm^{-1} , respectively. (c) Theoretical spots of the electron diffraction pattern along [012] zone axis.

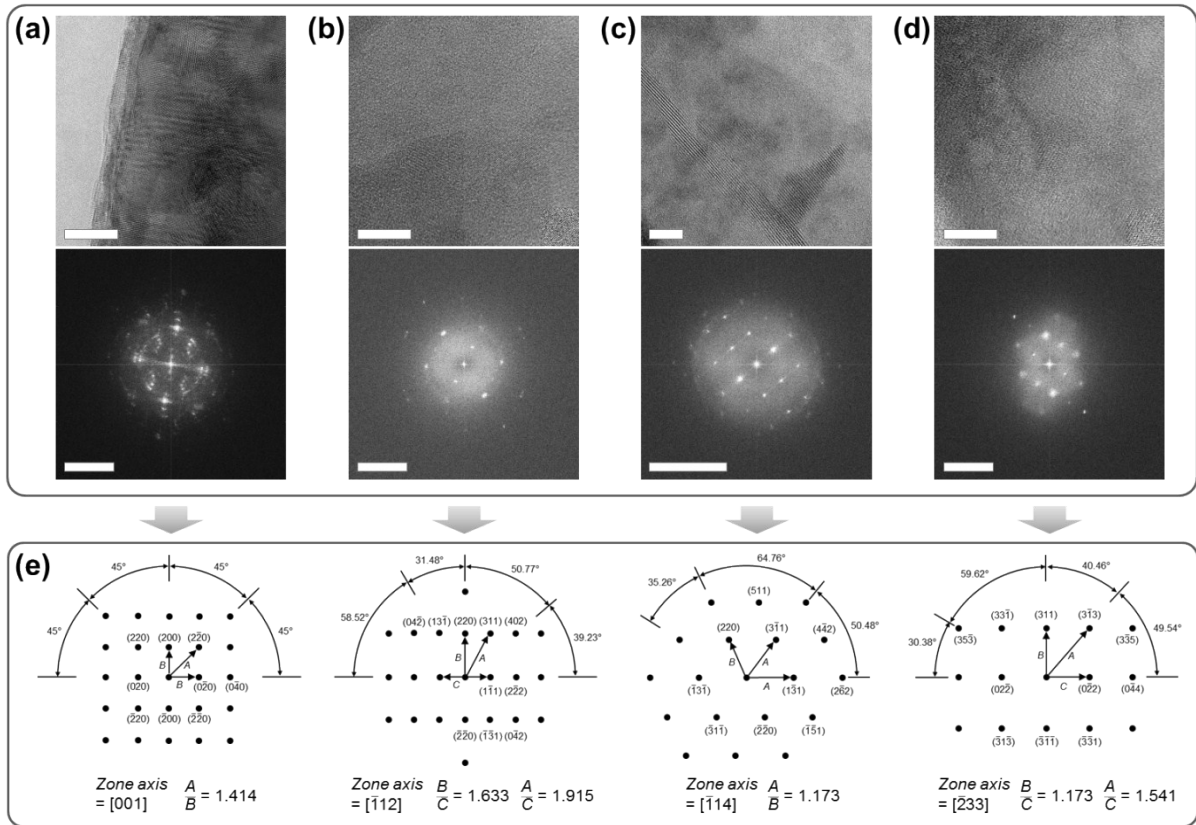


Fig. S10 HRTEM and FFT images of P(Py:BPDSA:Py)-GO measured along different zone axes. (a) [001] direction; (b) [-112] direction; (c) [-114] direction; (d) [-233] direction. Scale bars, 10 nm, and 5 nm^{-1} (for HRTEM and FFT pattern images, respectively). (e) Theoretical spots of electron diffraction patterns of the FCC structure. Several zone axes were slightly tilted due to the mobility of graphene oxide sheets during measuring. However, the information of all lattices is almost similar to their theoretical values.

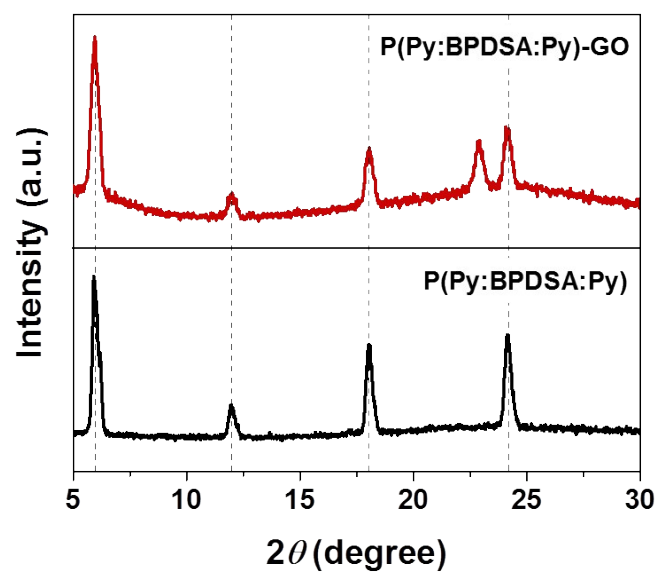


Fig. S11 XRD spectra of P(Py:BPDSA:Py)-GO and pure P(Py:BPDSA:Py). The crystalline characteristic peaks of P(Py:BPDSA:Py)-GO corresponds to those of pure P(Py:BPDSA:Py) having the d spacings in the [100] direction.

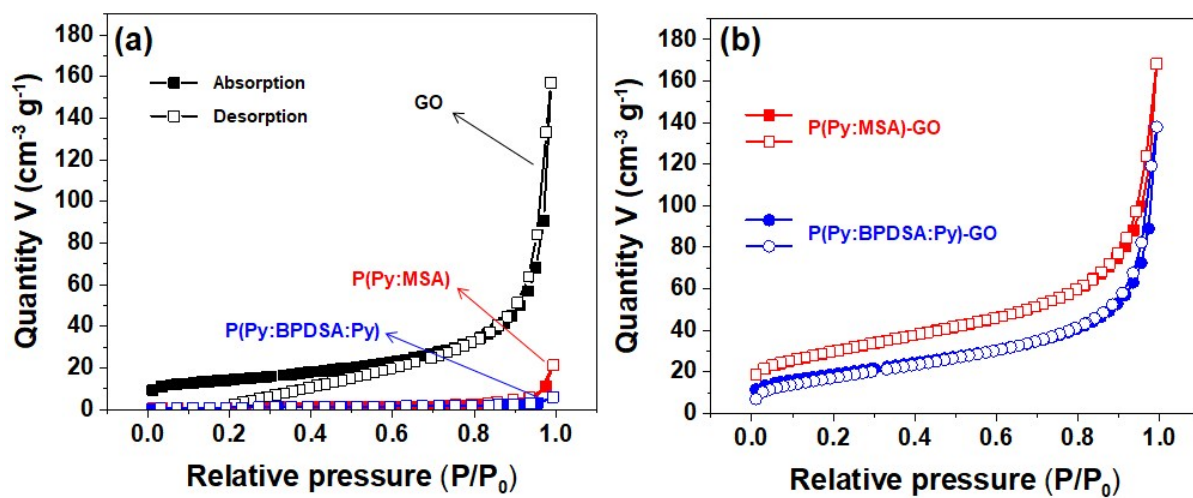


Fig. S12 N_2 adsorption/desorption isotherms: (a) GO, P(Py:MSA) and P(Py:BPDSA:Py). (b) P(Py:MSA)-GO and P(Py:BPDSA:Py)-GO.

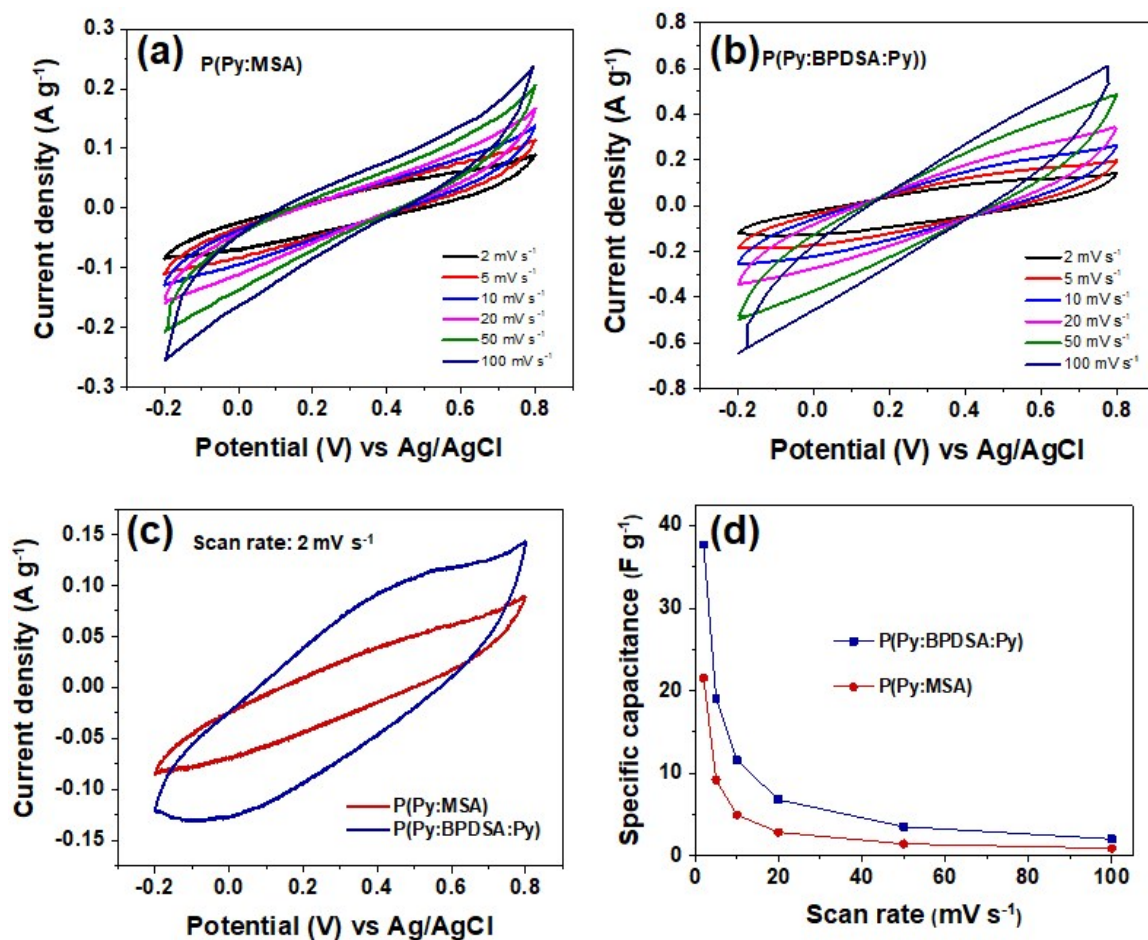


Fig. S13 Electrochemical performance of P(Py:MSA) and P(Py:BPDSA:Py). CV curves of P(Py:MSA) (a) and P(Py:BPDSA:Py), (b) at various scan rates, (c) CV curves of P(Py:MSA) and P(Py:BPDSA:Py) at a scan rate of 2 mV s⁻¹, and (d) specific capacitances of P(Py:MSA) and P(Py:BPDSA:Py) at various scan rates.

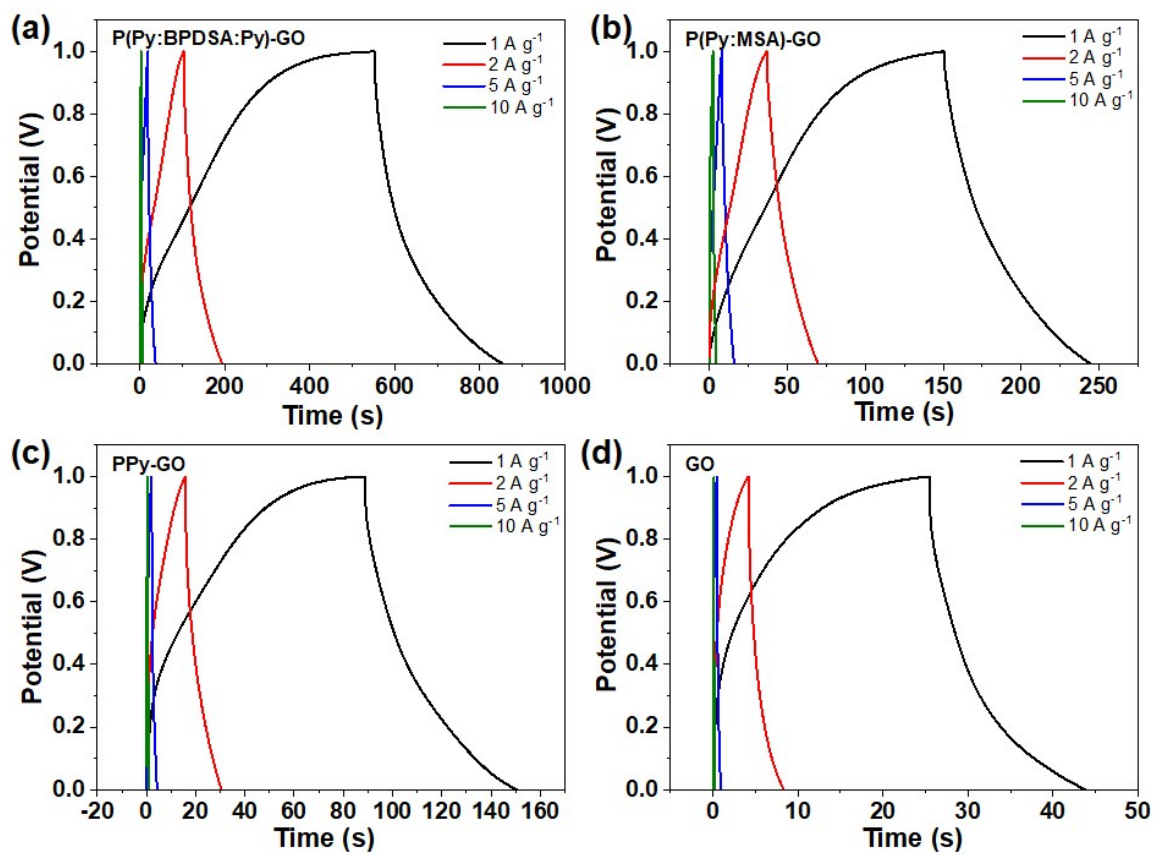


Fig. S14 Galvanostatic charge/discharge curves of (a) P(Py:BPDSA:Py)-GO, (b) P(Py:MSA)-GO, (c) PPy-GO and GO at various current density.

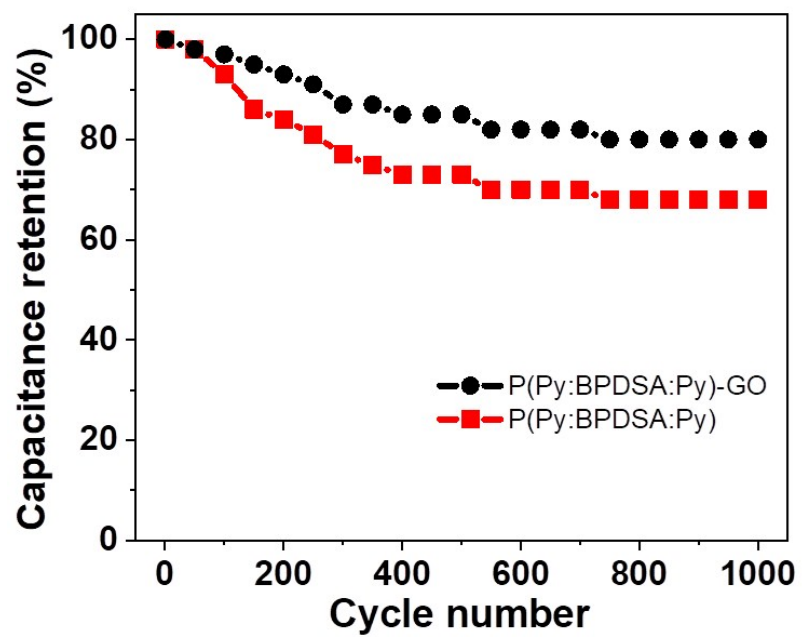


Fig. S15 Cyclic stability of P(Py:BPDSA:Py)-GO and P(Py:BPDSA:Py) for 1000 cycles at a scan rate of 10 mV s^{-1} .

Table S1. The capacitance of the similar materials reported in the literature.

Active material	Electrolyte	Scan rate or current density	Specific capacitance (F g ⁻¹)	Reference
P(Py:BPDSA:Py)/Graphene oxide	1 M H ₂ SO ₄	2 mV s ⁻¹	480	This work
PPy/Graphene	1 M H ₂ SO ₄	2 mV s ⁻¹	318	5
PPy/Graphene	3 M KCl	0.2 A g ⁻¹	255	6
Free-standing PPy/Graphene	1 M KCl	3 mA	278	7
PPy/rGO	1 M Li ₂ SO ₄	5 mV s ⁻¹ ,	114	8
PPy/rGO	3 M KCl	0.2 A g ⁻¹	290	9
PPy/rGO-CTAB	1 M H ₂ SO ₄	0.5 A g ⁻¹	324	10
PPy/Sulfonated graphene	1 M H ₂ SO ₄	1 A g ⁻¹	360	11
PPy/Graphene foam	3 M NaClO ₄	1.5 A g ⁻¹	350	12
PPy nanofiber/Graphene	1 M Li ₂ SO ₄	0.5 A g ⁻¹	161	13
PPy/N-doped graphene	6M KOH	2 mV s ⁻¹ .	393	14
PPy/Holy-GO	1M KOH	0.2 A g ⁻¹	418	15
Polyaniline/Graphene	1 M H ₂ SO ₄	1 A g ⁻¹	452	16
Polyaniline/Graphene/polyaniline	1 M H ₂ SO ₄	0.5 A g ⁻¹	384	17
e				
Polyaniline/rGO	1 M H ₂ SO ₄	0.45 A g ⁻¹	431	18

References

1. J. Cao, Y. Wang, J. Chen, X. Li, F. C. Walsh, J.-H. Ouyang, D. Jia and Y. Zhou, *J. Mater. Chem. A*, 2015, **3**, 14445-14457.
2. L. Atanasoska, K. Naoi and W. H. Smyrl, *Chem. mater.*, 1992, **4**, 988-994.
3. P. Patnaik and J. A. Dean, *Dean's analytical chemistry handbook*, McGraw-Hill, 2004.
4. H.-J. Lee, Y.-R. Jo, S. Kumar, S. J. Yoo, J.-G. Kim, Y.-J. Kim, B.-J. Kim and J.-S. Lee, *Nat. Commun.*, 2016, **7**, 12803.
5. C. Xu, J. Sun and L. Gao, *J. Mater. Chem.*, 2011, **21**, 11253-11258.
6. J. Zhu, Y. Xu, J. Wang, J. Wang, Y. Bai and X. Du, *Phys. Chem. Chem. Phys.*, 2015, **17**, 19885-19894.
7. H. P. De Oliveira, S. A. Sydlik and T. M. Swager, *The Journal of Physical Chemistry C*, 2013, **117**, 10270-10276.
8. C. Zhao, K. Shu, C. Wang, S. Gambhir and G. G. Wallace, *Electrochim. Acta*, 2015, **172**, 12-19.
9. J. Zhu and Y. Xu, *Electrochim. Acta*, 2018, **265**, 47-55.
10. X. Fan, Z. Yang and N. He, *RSC Advances*, 2015, **5**, 15096-15102.
11. C. Bora, J. Sharma and S. Dolui, *The Journal of Physical Chemistry C*, 2014, **118**, 29688-29694.
12. Y. Zhao, J. Liu, Y. Hu, H. Cheng, C. Hu, C. Jiang, L. Jiang, A. Cao and L. Qu, *Advanced materials*, 2013, **25**, 591-595.
13. K. Shu, Y. Chao, S. Chou, C. Wang, T. Zheng, S. Gambhir and G. G. Wallace, *ACS Appl. Mater. Interfaces*, 2018, **10**, 22031-22041.
14. L. Lai, L. Wang, H. Yang, N. G. Sahoo, Q. X. Tam, J. Liu, C. K. Poh, S. H. Lim, Z. Shen and J. Lin, *Nano Energy*, 2012, **1**, 723-731.
15. Y. He, Y. Bai, X. Yang, J. Zhang, L. Kang, H. Xu, F. Shi, Z. Lei and Z.-H. Liu, *J. Power Sources*, 2016, **317**, 10-18.
16. S. Gao, P. Zang, L. Dang, H. Xu, F. Shi, Z. Liu and Z. Lei, *J. Power Sources*, 2016, **304**, 111-118.
17. Z. Tong, Y. Yang, J. Wang, J. Zhao, B.-L. Su and Y. Li, *J. Mater. Chem. A*, 2014, **2**, 4642-4651.
18. M. Kim, C. Lee and J. Jang, *Adv. Funct. Mater.*, 2014, **24**, 2489-2499.